Kinetics of Reactions of Cl Atoms with Methane and Chlorinated Methanes

Mikhail G. Bryukov, Irene R. Slagle, and Vadim D. Knyazev*

Research Center for Chemical Kinetics, Department of Chemistry, The Catholic University of America, Washington, D.C. 20064

Received: March 19, 2002; In Final Form: June 4, 2002

The reactions of Cl atoms with methane and three chlorinated methanes (CH_3Cl, CH_2Cl_2, and $CHCl_3$) have been studied experimentally using the discharge flow/resonance fluorescence technique over wide ranges of temperature and at pressures between 1.4 and 8.8 Torr. The rate constants were obtained in direct experiments as functions of temperature: $k_1(Cl + CH_4) = 1.30 \times 10^{-19}T^{2.69} \exp(-497\ K/T)$ (295−1104 K), $k_2(Cl + CH_3Cl) = 4.00 \times 10^{-14}T^{0.92} \exp(-795\ K/T)$ (300−843 K), $k_3(Cl + CH_2Cl_2) = 1.48 \times 10^{-16}T^{1.58} \exp(-360\ K/T)$ (296−790 K), and $k_4(Cl + CHCl_3) = 1.19 \times 10^{-16}T^{1.51} \exp(-571\ K/T)$ (297−854 K) cm^3 $molecule^{-1}$ s^{-1}. Results of earlier experimental and theoretical studies of the reactions of Cl atoms with methane and chloromethanes are analyzed and compared with the results of the current investigation. It is demonstrated that the existing theoretical models of reactions 2−4 are in disagreement with the experiments and thus are not suitable for use in extrapolating the experimental results to conditions outside the experimental ranges. Thus, no better alternative to the use of experimental modified Arrhenius fits can be proposed at this time. A transition-state theory model of reaction 1 ($Cl + CH_4$) was created on the basis of ab initio calculations and analysis of the experimental data and was used to extrapolate the latter to temperatures outside the experimental ranges. The model results in the expression $k_1(Cl + CH_4) = 5.26 \times 10^{-19}\ T^{2.49} \exp(-589\ K/T)$ cm^3 $molecule^{-1}$ s^{-1} (200−3000 K) for the temperature dependence of the rate constant. Temperature dependences of the rate constants of the reverse $R + HCl \rightarrow Cl + RH$ reactions were derived on the basis of the experimental data, modeling, and thermochemical information.

I. Introduction

Chlorinated hydrocarbons (CHCs) are recognized as toxic, persistent, and biocumulative chemicals. As such, incineration has become the disposal method of choice for these environmentally hazardous wastes. However, the products of incomplete combustion of organochlorine compounds (e.g., phosgene) may be more harmful than the initial waste. Key to the understanding of CHC combustion and its products is fundamental knowledge of the mechanisms, specific pathways, and rate constants of the important elementary reactions involved. Among the most important and sensitive reactions involved in the currently used mechanisms of the combustion of chlorinated hydrocarbons are the reactions of Cl and H atoms with the main compounds that are being burned.[1−9] In CHC/O_2 and $CHC/hydrocarbon/O_2$ flames, reactions of Cl and H atoms with CHCs together with unimolecular decomposition are the major channels of consumption of CHCs.[1−5,7−14] The results of numerical simulations demonstrate that the rates of CHC destruction and the concentrations of active species are highly sensitive to the rates of Cl + CHC and H + CHC reactions.

As part of a project directed at the elucidation of the kinetics of these important reactions, we recently reported[15,16] the results of our experimental and computational studies of the reactions of H atoms with methane, four chlorinated methanes, ethane, and three chlorinated ethanes. In the current work, we extend such kinetic studies to the reactions of Cl atoms with methane and three chlorinated methanes conducted over wide ranges of temperature.

$$Cl + CH_4 \rightarrow HCl + CH_3 \qquad (295-1104\ K) \qquad (1)$$

$$Cl + CH_3Cl \rightarrow HCl + CH_2Cl \qquad (300-843\ K) \qquad (2)$$

$$Cl + CH_2Cl_2 \rightarrow HCl + CHCl_2 \qquad (296-790\ K) \qquad (3)$$

$$Cl + CHCl_3 \rightarrow HCl + CCl_3 \qquad (297-854\ K) \qquad (4)$$

Numbers in parentheses indicate the experimental temperature ranges of the current work.

Reaction 1 has received ample attention from researchers (refs 17−30 and references therein), with generally good agreement between low-temperature results obtained by direct and indirect methods. Reviews of these data can be found, for example, in refs 18, 31−34. However, the only two direct studies of reaction 1 conducted above 500 K (Clyne and Walker,[17] 300−686 K; Pilgrim et al.,[30] 292−800 K) reported rate constants that differ from each other by approximately a factor of 2 over the 500−686 K temperature interval. The current study extends the temperature range of direct experimental study of reaction 1 to 1104 K.

Although reactions 2−4 have been studied before, most of the studies either involved indirect determinations of rate constants and/or were confined to low temperatures, where research was stimulated by the importance of these reactions to atmospheric chemistry. Despite the substantial number of experimental studies (see refs 17, 22, 31, 34−46 and references

* Corresponding author. E-mail: knyazev@cua.edu.

10.1021/jp0257909 CCC: $22.00
Published on Web 10/15/2002

therein), there is no accord between the results of these investigations. The differences in the room-temperature rate constants are as large as nearly an order of magnitude (reaction 4, refs 17 and 43). There is no agreement between the direct rate constant determinations of reactions 2 (refs 17 and 22, a factor of 6 difference in the preexponential factor and 4 kJ mol^{-1} in the activation energy) and 4 (refs 17 and 45, a factor of 4 difference).

In the current study, the kinetics of reactions 1−4 was investigated by the discharge flow technique with resonance fluorescence detection of Cl atoms. The excellent sensitivity of the method (detection limit of $<10^8$ atoms cm^{-3}) permits us to conduct experiments with very low initial Cl concentrations ($\leq 10^{11}$ atoms cm^{-3}), thus ensuring the absence of any complications due to potential fast secondary reactions. Rate constants of reactions 1−4 were obtained as functions of temperature in direct experiments.

The article is organized as follows. Section I (current) is an introduction. The experimental method, procedures, and results are reported in section II. The results are discussed in section III, where a transition-state theory model of reaction 1 is also presented and rate constants of the reverse reactions are calculated. Brief conclusions are given in section IV.

II. Experimental Section

Rate constant measurements were conducted in a heatable tubular flow reactor under pseudo-first-order conditions with a large excess of molecular substrate. Cl atoms were detected by resonance fluorescence, and their decay was measured as a function of contact time over a wide range of experimental conditions.

II.1. Experimental Apparatus. Details of the experimental apparatus have been described previously in connection with our investigations of the reactions of H atoms.[15,16] In the current work, the apparatus was modified to enable us to study Cl atom reactions. A brief description of the apparatus and recent modifications is given below. Cl atoms were generated in the sidearm of a heated tubular quartz reactor by a 2.45-GHz microwave discharge in a Cl_2/He mixture. Chlorine atoms formed in the discharge area were carried through the reactor by a flow of helium, and their concentration was monitored by resonance fluorescence in the detection zone located downstream. The molecular substrate (CH_xCl_y) was introduced through a quartz movable injector.

Various aspects of the discharge flow technique of measuring rate constants of gas phase chemical reactions have been extensively discussed in the literature.[47−50] These discussions are not repeated here. Care was taken to ensure that, under all experimental conditions used in the current work, the plug-flow approximation was valid. The only exception to the plug-flow approximation was the minor contribution of axial and radial diffusion of Cl atoms. Corrections for axial and radial diffusion had to be introduced into the experimentally obtained atom decay rates (vide infra). The range of typical values of the viscous pressure drop in the working part of the heated zone was 0.03−0.15 Torr. The uniformity of the temperature profiles in this region (15−30 cm in length) was at least 6 K (maximum temperature differences were 6 K at 1104 K and not more than 0.5% of T at lower temperatures).

Two quartz reactors with different internal diameters (1.93- and 3.19-cm i.d.) were used in these experiments. The reactor surface, the surface of the movable injector, and the inside of the discharge tube were treated to reduce the heterogeneous loss of Cl atoms by first soaking in a 5% aqueous solution of ammonium bifluoride for 30 min with subsequent rinsing with distilled water and then by the method of Sepehrad et al.[51] The resultant values of the first-order wall loss rate constant, k_w, were always below 20 s^{-1}. Typical values of k_w were ∼2−7 s^{-1}. Reactors of different diameters were used to rule out potential contributions of heterogeneous reactions to the rate constant values obtained in the experiments (vide infra). It was reported in a number of publications that the rates of Cl atom loss on the surface of uncoated glass or quartz can reach rather large values (e.g., ref 52). Our findings proved to the contrary: the surface treatment described above, which is essentially a very thorough cleaning of the quartz surface, resulted in low Cl atom wall losses.

Cl atom resonance fluorescence was induced by light from a discharge flow resonance lamp[53,54] and was detected by a solar blind photomultiplier (EMR model 542-G-09, peak of sensitivity in the 115−170-nm spectral interval). CaF_2 windows (cutoff 123 nm) and a gas optical filter (1 Torr of N_2O, optical path length 3 cm)[54,55] are used to block potential radiation from H and O atoms (121.6 and 130.2−130.6 nm, respectively) while transmitting the Cl resonance lines at 135−139 nm. The sensitivity of the atom detection system to Cl atoms was determined by titration with Br_2 (the rate constant of the Cl + Br_2 reaction is $\geq 10^{-10}$ cm^3 $molecule^{-1}$ s^{-1}).[56,57] The sensitivity limit (defined by the unity signal-to-noise ratio) was $<10^8$ atom cm^{-3}.

Molecular substrates (CH_xCl_y) were stored undiluted in Pyrex reservoirs. Flows of these reagents into the reactor were determined by measuring the pressure drop over time in a calibrated volume. That the measured flows were independent of the surface-to-volume ratio of the calibrated volume was verified to ensure the absence of interference from heterogeneous absorption and desorption processes on the walls of the vacuum manifold. Flows of molecular chlorine to the atom-producing discharge were measured in a similar way. The dissociation efficiency of the discharge was in the 20−50% range, which resulted in the concentrations of undissociated Cl_2 in the reactor being no more than a factor of 2 higher than the initial Cl atom concentrations.

A flow of CF_4 with concentrations in the $(2.5-33.4) \times 10^{14}$ molecule cm^{-3} range was added to the carrier gas through an inlet located upstream from the reaction zone in order to ensure fast equilibration[27] of the ground and the excited spin−orbit states of the Cl atom. Literature values of the room-temperature quenching rate coefficient range from $(0.23-1.5) \times 10^{-10}$ cm^3 $molecule^{-1}$ s^{-1}.[58−60] Therefore, the large concentrations of CF_4 used in the current work ensure that the rate of spin−orbit equilibration is much faster than the rates of the reactions under study.

II.2. Reaction Rate Measurements. All experiments to measure the rate constants of reactions 1−4 were conducted under conditions of a large excess of molecular substrate ($39 \leq [CH_xCl_y]/[Cl]_0 \leq 1.2 \times 10^5$). Initial concentrations of Cl atoms in the detection zone were in the range of $(1-9) \times 10^{10}$ atoms cm^{-3}. Exact knowledge of the Cl atom concentrations is not needed for the determination of rate constants because all experiments were conducted under pseudo-first-order conditions. The rate of heterogeneous loss of Cl atoms on the walls of the reactor and the movable injector (2−17 s^{-1}) was regularly measured (in the absence of molecular substrate). In these measurements, the time of contact between the Cl atoms generated in the discharge and the walls was varied by changing the flow velocity (by switching the flow of helium carrier gas between a fixed inlet located near the Cl atom source and the

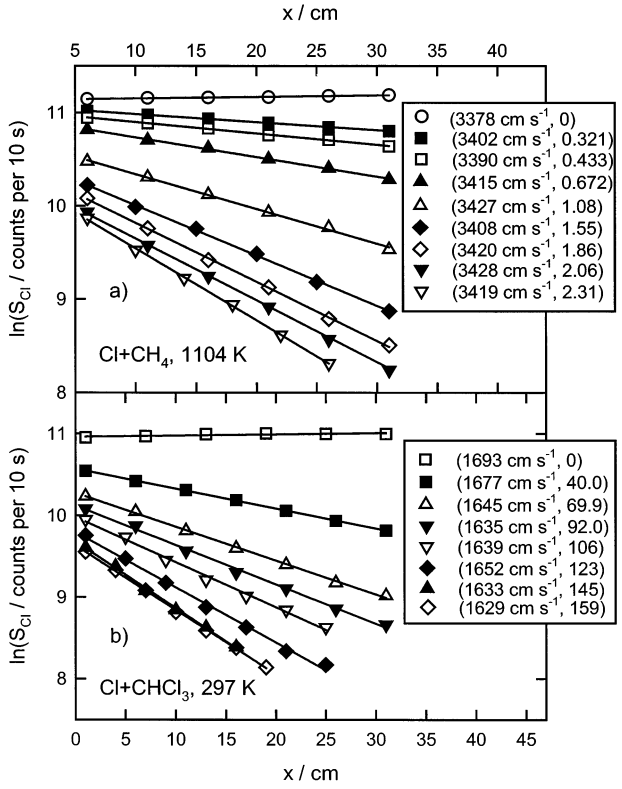

Figure 1. Examples of experimentally obtained ln(S_{Cl}) vs x dependences. Data from experiment 13 on Cl + CH_4 and experiment 1 on Cl + $CHCl_3$ (see Table 1). Numbers in parentheses are the flow velocities and concentrations of the CH_xCl_y substrate (10^{13} molecules cm^{-3}).

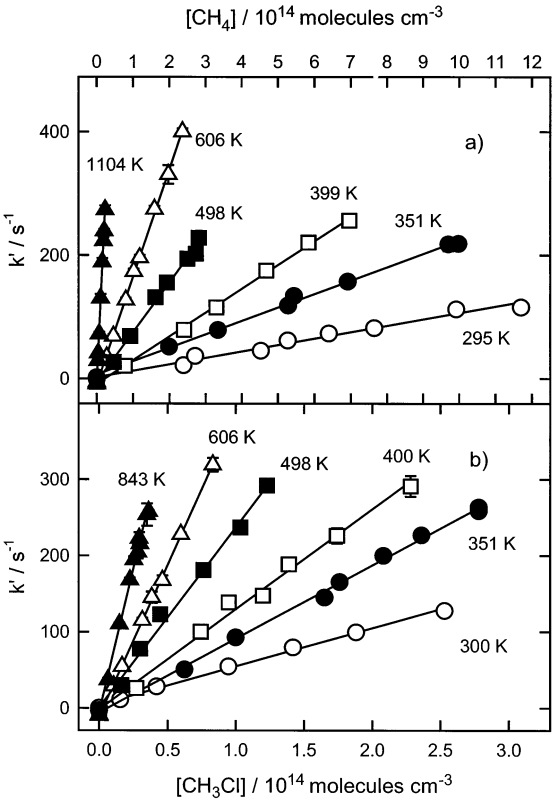

Figure 2. Examples of experimentally obtained k' vs [CH_4] (a) and k' vs [CH_3Cl] (b) dependences. Experimental temperatures are indicated on the plots.

movable injector at various positions of the latter) with no alterations of the conditions in the discharge and monitoring the resultant changes in the signal of Cl atoms in the detection zone.

The time of contact between the molecular substrate and Cl atoms was varied by changing the position of the movable injector. Under the experimental conditions used, plug-flow conditions are satisfied (except for a required minor correction for axial and radial diffusion, vide infra), and increments of contact time can be obtained by dividing the corresponding changes in the length of the contact zone by the bulk flow velocity, V. The tip of the movable injector was always kept within the heated working zone of the reactor.

The total signal (counts s^{-1}) detected by the photomultiplier consisted of three components: fluorescence of Cl atoms (S_{Cl}), the photomultiplier dark current (less than 1 count s^{-1}), and the scattered light originating from the resonance lamp and reflected by the walls of the detection system (typically ~1000 counts s^{-1}). The contributions from the dark current and the scattered light were measured directly in the absence of Cl atoms but with the molecular substrate present (to account for possible absorption of the scattered light) and were later subtracted from the total signal to obtain S_{Cl}.

The effective first-order rate constant values, k'_{obs}, were obtained from least-squares fits of the Cl atom fluorescence signal S_{Cl} to the equation

$$\ln(S_{Cl}) = \text{constant} - k'_{obs} x V^{-1} \qquad \text{(I)}$$

where x is the distance between the tip of the movable injector and the detection zone and V is the bulk flow velocity in the reactor. Examples of experimentally obtained ln(S_{Cl}) versus x dependences are presented in Figure 1. The observed values of k'_{obs} were corrected for axial and radial diffusion of Cl atoms via the equation[47,49,61]

$$k' = k'_{obs}\left(1 + \frac{k'_{obs} D}{V^2} + \frac{k'_{obs} R^2}{48D}\right) \qquad \text{(II)}$$

where D is the diffusion coefficient of Cl atoms in He and R is the reactor radius. The values of D were calculated using the

$$D = 0.0237 T^{1.75} \text{ Torr cm}^2 \text{ s}^{-1} \qquad \text{(III)}$$

equation.[62] This correction for atom diffusion never exceeded 8% of the final value of k'.

The bimolecular rate constants of reactions 1−4 were obtained from the slopes of the linear dependences of k' on the concentration of substrate, [CH_xCl_y]:

$$k' = k_i [CH_xCl_y] + k_0 \qquad \text{(IV)}$$

Here, k_i is the bimolecular rate constant of the reaction under study (i = 1−4), and k_0 is the zero-abscissa intercept of the k' versus [CH_xCl_y] dependence. The k_0 intercept appears because of the nonnegligible losses of Cl atoms on the surfaces of the reactor and the movable injector and can acquire both positive and negative values.[15] The values of k_0 obtained in the current study were minor compared with the first term in eq IV (see Table 1), and uncertainties in k_0 were generally comparable with the k_0 values. Examples of experimentally obtained k' versus [CH_xCl_y] dependences are presented in Figures 2 and 3. The upper limits of the experimental temperature ranges for reactions 2−4 were determined by the onset of thermal decomposition of the CH_xCl_y substrates.

Gases used in the experiments were obtained from MG Industries (He, >99.9999%, CF_4, >99.9%), Aldrich (CH_3Cl,

TABLE 1: Conditions and Results of Experiments to Measure the Rate Constants of the Reactions of Cl Atoms with Methane and Chlorinated Methanes

no.[a]	T/K	P/Torr[b]	$[CH_xCl_y]$[c] range/10^{12}	$[CF_4]$[c]/10^{14}	k_0/s^{-1} [d]	V/cm s^{-1} [e]	$[Cl]_0$[c]/10^{10}	$((k' - k'_{obs})/(k'_{obs}))_{max}$ [f]	k_i [g]/10^{-13}
				$Cl + CH_4 \rightarrow HCl + CH_3$ (1)					
1*	295	1.36−1.38	239−1170[h]	21	2.4 ± 7.5	842−853	3.0	0.069	1.04 ± 0.11
2	298	4.70−4.74	661−2380	23	−4.6 ± 7.1	2560−2614	5.9	0.047	1.084 ± 0.055
3	300	6.06−6.09	175−1180	19	−5.2 ± 4.6	2073−2104	2.1	0.033	1.190 ± 0.067
4	351	5.54−5.58	199−998	15	6.4 ± 6.6	2682−2704	2.6	0.037	2.18 ± 0.11
5	399	6.09−6.16	77.3−696	10	−8.6 ± 5.6	2587−2607	3.1	0.038	3.85 ± 0.13
6	498	6.07−6.11	46.5−281	10	−5.3 ± 9.7	2588−2631	2.4	0.028	8.06 ± 0.51
7	606	8.70−8.73	27.4−197	18	−9.8 ± 4.7	2831−2895	4.5	0.038	17.48 ± 0.36
8*	704	3.86−3.87	11.0−83.6[h]	5.2	−0.9 ± 5.6	2703−2734	3.7	0.044	31.2 ± 1.1
9	777	8.76−8.79	9.6−103	18	−14 ± 12	2917−2964	5.4	0.037	40.2 ± 1.8
10	843	8.79−8.80	10.2−77.6	20	−17 ± 11	3150−3175	2.9	0.036	55.7 ± 2.4
11	909	8.78−8.80	12.7−64.7	22	−8.0 ± 9.0	2874−3060	5.8	0.033	60.0 ± 2.4
12*	1012	5.16−5.19	4.54−24.4[h]	2.5	−3 ± 10	2661−2684	3.5	0.043	105.6 ± 6.9
13*	1104	3.93−3.95	3.21−23.1	8.5	−7.7 ± 5.4	3378−3428	8.2	0.039	122.8 ± 3.9
				$Cl + CH_3Cl \rightarrow HCl + CH_2Cl$ (2)					
1*	300	2.49−2.49	15.4−253	13	4.6 ± 4.1	1075−1085	8.8	0.053	5.01 ± 0.30
2	300	6.04−6.08	64−471	18	−1.0 ± 5.5	1982−2022	3.4	0.061	5.47 ± 0.20
3*	324	2.96−2.97	19.7−273[i]	6.9	8.0 ± 8.3	1207−1219	4.0	0.077	7.39 ± 0.54
4	351	5.49−5.51	62.3−278	20	−5.9 ± 6.7	2616−2644	8.9	0.044	9.66 ± 0.35
5	400	6.08−6.12	27.2−228	10	−1.6 ± 12	2616−2652	5.2	0.045	13.13 ± 0.94
6	498	6.07−6.08	16.1−123	14	1 ± 12	2679−2704	9.0	0.035	23.6 ± 1.8
7	606	8.73−8.75	10.7−83.1	15	−11.2 ±3.4	2886−2956	2.0	0.037	39.80 ± 0.78
8	701	6.16−6.17	12.2−51.84	13	−18 ± 10	2747−2769	2.2	0.026	54.5 ± 3.1
9*	790	4.06−4.09	8.93−37.1	9.7	2.3 ± 9.6	3059−3101	4.4	0.036	68.5 ± 3.7
10	843	8.74−8.78	6.44−36.1	14	−5.9 ± 9.0	3098−3138	7.7	0.023	75.6 ± 3.5
				$Cl + CH_2Cl_2 \rightarrow HCl + CHCl_2$ (3)					
1	296	6.11−6.15	97.0−350	31	0.3 ± 5.4	2439−2482	1.0	0.030	3.40 ± 0.22
2	297	3.70−3.73	44.6−544	8.9	5.0 ± 7.9	2817−2863	1.5	0.030	3.52 ± 0.24
3*	297	1.91−1.94	13.9−463	8.1	6.6 ± 3.8	978−989	4.8	0.077	3.68 ± 0.17
4	344	5.22−5.25	46.6−323	20	−0.4 ± 9.3	2928−2994	4.0	0.015	5.27 ± 0.48
5	397	5.21−5.24	70.1−258	14	4.7 ± 9.2	2992−3039	4.8	0.019	8.10 ± 0.56
6	507	7.20−7.28	26.1−133	28	5.1 ± 7.2	2592−2633	3.0	0.023	13.36 ± 0.90
7	566	6.62−6.69	25.5−198	6.7	−3.0 ± 14.0	4003−4097	1.9	0.029	16.3 ± 1.2
8*	605	4.03−4.04	18.4−105	5.7	8.0 ± 7.6	2361−2404	6.0	0.042	21.2 ± 1.4
9*	705	4.02−4.03	12.2−102[j]	6.8	11.0 ±12.0	2765−2786	2.3	0.046	28.8 ± 2.2
10*	790	4.07−4.08	7.8−71.7	18	−12.8 ± 5.6	3001−3057	7.2	0.036	35.3 ± 1.4
				$Cl + CHCl_3 \rightarrow HCl + CCl_3$ (4)					
1	297	7.85−8.17	400−1590	33	2.3 ± 9.7	1629−1693	1.3	0.043	0.891 ± 0.092
2	344	5.21−5.41	242−1330	9.1	9 ± 11	2866−2973	4.4	0.037	1.69 ± 0.13
3	397	6.21−6.37	142−835	24	2.0 ± 6.3	2747−2834	1.8	0.032	2.40 ± 0.13
4	510	6.76−6.92	119−616	18	−1.1 ± 7.9	3489−3545	1.6	0.031	4.30 ± 0.22
5	557	4.31−4.44	84.9−418	6.4	4.9 ± 5.4	3026−3118	6.5	0.023	5.88 ± 0.25
6*	605	4.00−4.03	42.1−282	6.3	2.6 ± 3.2	2342−2401	8.0	0.041	7.58 ± 0.20
7*	705	4.02−4.04	40.7−218	11	−1.9 ± 5.3	2716−2764	3.5	0.038	11.12 ± 0.42
8*	790	4.05−4.08	8.5−197	3.0	3.3 ± 4.2	3048−3103	8.0	0.037	13.21 ± 0.44
9*	854	4.07−4.10	14.6−148	11	6.8 ± 5.8	3274−3318	3.3	0.036	16.58 ± 0.69

[a] Experiment number. A reactor with an internal diameter (i.d.) of 3.19 cm was used in experiments marked with *, and a reactor with i.d. = 1.93 cm was used in unmarked experiments. [b] Minor variations in pressure are due to changes in flow conditions upon the addition of large flows of molecular substrate (CH_xCl_y). [c] Units of concentration are molecule cm^{-3}. [d] Zero-abscissa intercept on the k' versus $[CH_xCl_y]$ dependence (see discussion of eq IV in the text). [e] Bulk flow velocity range. Minor variations in flow velocity are due to changes in flow conditions upon the addition of large flows of molecular substrate (CH_xCl_y). [f] Maximum relative value of the diffusion correction via eq II. [g] Units of rate constants are cm^3 molecule^{-1} s^{-1}. Error limits represent statistical uncertainties and are reported as 2σ. Maximum estimated systematic uncertainties are 8% of the rate constant value (see text). [h] A sample of CH_4 with purity >99.999% obtained from Matheson was used. The CH_4 sample obtained from Aldrich (>99.99%) was used in all other experiments on reaction 1. [i] A sample of CH_3Cl obtained from Aldrich (purity ≥99.9% according to certificate of analysis) was used. The CH_3Cl sample obtained from Matheson (purity after vacuum distillation ≥99.98% as verified by GC analysis) was used in all other experiments on reaction 2. [j] A sample of CH_2Cl_2 obtained from Aldrich (stabilized with 50−150 ppm cyclohexene) was used. The CH_2Cl_2 sample obtained from Fluka (20 ppm impurity of *trans*-2-pentene) was used in all other experiments on reaction 3.

≥99.5%; CH_2Cl_2, ≥99.9%; $CHCl_3$, ≥99.99%), Fluka (CH_2Cl_2, ≥99.9%), and Matheson (CH_4, ≥99.99%; CH_3Cl, ≥99.5%). The indicated purity values are nominal, as specified by the manufacturer. All gases except helium were purified by vacuum distillation prior to use. Helium was purified by passing through liquid-nitrogen-cooled traps. To verify that no potential impurities in the methane or chlorinated methanes could affect the measured rate constants, these gases were analyzed for potential contaminants by gas chromatography. After purification by vacuum distillation, the purity of all chloromethanes significantly exceeded the specifications provided by the manufacturers. A discussion of impurities and their potential influence on the experimental results is given in the next subsection (II.3).

II.3. Results. The conditions and results of experiments to determine the values of the rate constants of reactions 1−4 are presented in Table 1. The rate constants demonstrate no dependence on pressure, the initial concentration of Cl atoms, bulk flow velocity, or the concentration of the CF_4 spin−orbit quencher within the experimental ranges. The fact that the rate constants are independent of the initial Cl atom concentration indicates the absence of any influence of potential secondary reactions on the kinetics of Cl atoms, as can be expected from

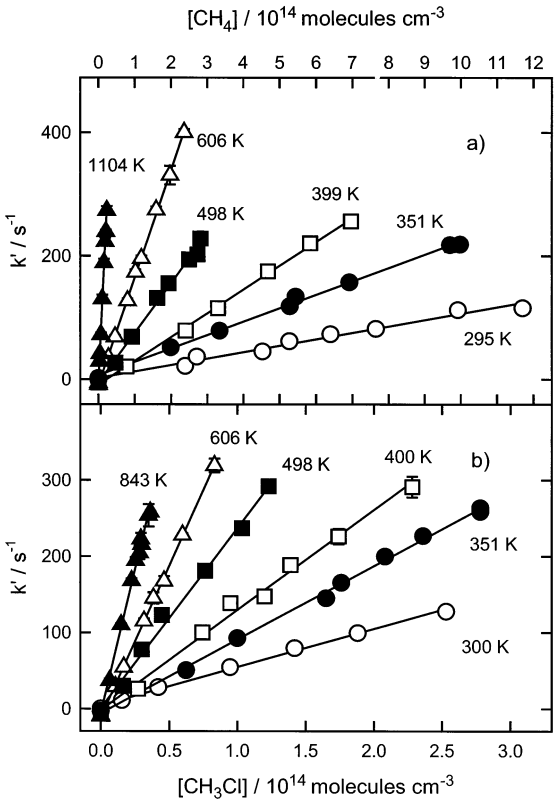

Figure 3. Examples of experimentally obtained k' vs $[CH_2Cl_2]$ (a) and k' vs $[CHCl_3]$ (b) dependences. Experimental temperatures are indicated on the plots.

the low values of $[Cl]_0$ used ($[Cl]_0 = (1-9) \times 10^{10}$ atoms cm^{-3}). Potential regeneration of Cl atoms through the secondary R + $Cl_2 \rightarrow$ RCl + Cl processes (rate constants 2×10^{-12} cm^3 molecule^{-1} s^{-1} or less[63−65]) is negligible because of the low Cl_2 concentrations ($<2 \times 10^{11}$ molecule cm^{-3}).

To ensure that the measured rates of Cl atom decay in the presence of CH_xCl_y represent the homogeneous reactions 1−4, experiments were conducted with reactors of different internal diameters (1.93−3.19 cm) possessing different surface-to-volume ratios. The experimentally obtained values of the rate constants were independent of the reactor used (Table 1). This independence, as well as the linearity of the observed k' versus $[CH_xCl_y]$ dependences, indicates the absence of any significant effects of heterogeneous reactions on the values of the rate constants.

The rate constants of reactions 1−4 exhibit positive temperature dependences (Figures 4−7) that can be represented with modified Arrhenius expressions within their corresponding experimental temperature ranges:

$$k_1 = 1.30 \times 10^{-19} T^{2.69} \exp(-497\ \mathrm{K}/T)\ \mathrm{cm^3\ molecule^{-1}\ s^{-1}} \quad (295-1104\ \mathrm{K})\ \ (\mathrm{V})$$

$$k_2 = 4.00 \times 10^{-14} T^{0.92} \exp(-795\ \mathrm{K}/T)\ \mathrm{cm^3\ molecule^{-1}\ s^{-1}} \quad (300-843\ \mathrm{K})\ \ (\mathrm{VI})$$

$$k_3 = 1.48 \times 10^{-16} T^{1.58} \exp(-360\ \mathrm{K}/T)\ \mathrm{cm^3\ molecule^{-1}\ s^{-1}} \quad (296-790\ \mathrm{K})\ \ (\mathrm{VII})$$

$$k_4 = 1.19 \times 10^{-16} T^{1.51} \exp(-571\ \mathrm{K}/T)\ \mathrm{cm^3\ molecule^{-1}\ s^{-1}} \quad (297-854\ \mathrm{K})\ \ (\mathrm{VIII})$$

The maximum deviations of the experimental rate constant values from the above parametrized expressions are 12% (expression V), 7% (expressions VI and VII), and 10% (expression VIII). Error limits of the parameters in expressions V−VIII are not presented here, as these parameters bear no physical meaning. It can be noted here that there exists a theoretical formalism for treating atom transfer reactions, which results in a modified Arrhenius expression with physically meaningful parameters.[66] This modified Arrhenius expression has a functional form that is different from that of expressions V−VIII and is based on the explicit factoring out of the contributions of tunneling, thermal vibrational excitation of the bending modes of the transitional Cl−H−R structure, and several other properties of the transition state. An analysis of the experimental $k(T)$ dependences via the formalism of ref 66 can be expected to yield fitted parameters with meaningful uncertainties. However, such an analysis (already performed in ref 66 for reaction 1 and a series of other reactions of H transfer) is beyond the scope of the current experimental study.

The error limits of the experimentally obtained values reported in this work (Table 1) represent 2σ statistical (random) uncertainty. The maximum estimated systematic uncertainty is 8% of the rate constant value.

To verify that no potential impurities in the chlorinated methanes could affect the measured rate constants, these gases were analyzed for potential contaminants by gas chromatography. A Shimadzu GC-9A gas chromatograph and a Hewlett-Packard 5890 II Plus/5989B GC/MS were used in these analyses. It was found that, after purification by vacuum distillation, the purity of all chloromethanes (CH_3Cl, >99.98%; CH_2Cl_2, >99.98%; $CHCl_3$, >99.999%) significantly exceeded the specifications provided by the manufacturers. For reactions 1−3, rate constant determinations were performed with methane and chloromethanes obtained from different commercial sources (see Table 1). One potential concern about purity of the samples of chlorinated methanes is related to the presence of small amounts of stabilizers (cyclohexene or *trans*-2-pentene in CH_2Cl_2 and $CHCl_3$). By considering the analogy with saturated hydrocarbons of this size,[67−69] reactions of Cl atoms with these molecules can be expected to have rate constants of $\sim(2-3) \times 10^{-10}$ cm^3 molecule^{-1} s^{-1}. The sample of dichloromethane used in most of the experiments had a 20 ppm impurity of *trans*-2-pentene, which could result in a maximum contribution of 1.7% to the measured rate constant of reaction 3 at the lowest experimental temperature. The sample of trichloromethane contained an impurity of 3 ppm of *trans*-2-pentene, as was demonstrated by GC/MS analysis. This impurity could result in a maximum contribution of 1% to the measured rate constant of reaction 4 at the lowest experimental temperature. The potential effects of impurities are expected to decrease with temperature since the fast Cl + impurity reactions are expected to show little or no increase with temperature. Therefore, impurity effects on the values of the rate constants obtained in the current study are negligible compared to the experimental uncertainties.

III. Discussion

III.1. Experimental Rate Constant Values. *Reaction Cl + CH_4 → HCl + CH_3 (1).* Reaction 1 has been studied previously at low temperatures with the results of several direct and indirect studies being in general agreement with each other (see, for example, refs 17−30). Reviews of these data ($T \leq$ 500 K) can be found in refs 18 and 31−34 and are not repeated here. The rate constants obtained in the current study agree with these earlier low-temperature measurements (Figure 4, low-temperature data are exemplified by refs 23 and 27). The only two direct studies of reaction 1 conducted above 500 K are those

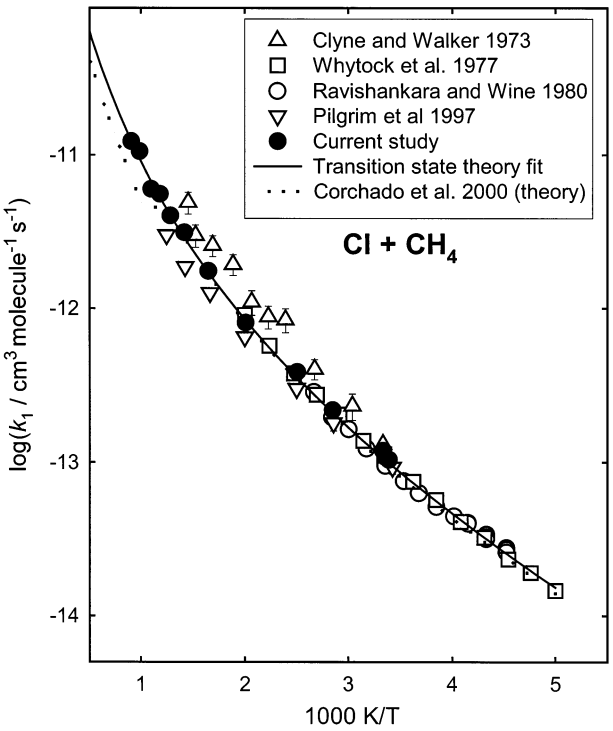

Figure 4. Temperature dependence of the rate constant of reaction 1. Results of only a few representative direct studies are displayed to avoid plot congestion: Clyne and Walker,[17] Whytock et al.,[23] Ravishankara and Wine,[27] Pilgrim et al.,[30] and the current study. Other directly obtained low-temperature data[18−20,22,26,29] are in general agreement with the results of refs 23 and 27. The solid line represents the transition-state theory fit. The dotted line (broken in the 800−1000 K region) shows the $k_1(T)$ dependence obtained in the theoretical study of Corchado et al.[73] (see text).

of Clyne and Walker[17] (300−686 K) and Pilgrim et al.[30] (292−800 K). In the experiments of Clyne and Walker, rate constants of reactions 1−4 were determined by the discharge flow technique with mass spectroscopic detection of the involved species. These experiments were conducted in large excess of Cl atoms over the CH_xCl_y molecular substrate. At temperatures above ambient, the results of ref 17 are larger that those of the current study and other studies included in Figure 4. Moreover, even stronger differences between the results of Clyne and Walker and those of other experimental investigations are observed in the cases of reactions 2−4 (vide infra), which arouses suspicion of potential systematic factors that could have affected the experiments in ref 17.

The experiments of Pilgrim et al. were performed using the 193-nm laser photolysis of CF_2Cl_2 to produce Cl atoms and long-path infrared absorption to detect the HCl formed in reaction 1. The results of ref 30 are somewhat lower than those obtained in the current study, with the difference reaching ~30% at $T \geq 500$ K. When compared with the results of Whytock et al. (which covered the 200−500 K temperature interval), the k_1 values of Pilgrim et al. are also lower by 28% at 500 K and 20% at 400 K. The initial concentrations of Cl atoms used in ref 30 were approximately 10^{12} atom cm^{-3},[70] an order of magnitude or more larger than those used in the current study. If any secondary reactions producing HCl occurred in the reactive system, then additional HCl would appear at longer reaction times (compared to the production of HCl in reaction 1). Such additional HCl production would have had the effect of extending the experimental characteristic rise time of the HCl signal and thus would have reduced the derived rate constants. One can suggest the reaction $CF_2Cl + CH_3 \rightarrow HCl + CH_2CF_2$[71] ($CF_2Cl$ radical coming from the photolysis of the Cl atom precursor, CF_2Cl_2) as potentially having such an effect. However, no deviations[70] from the exponential shapes of the well-resolved rising HCl profiles were observed in ref 30, which seems to contradict the secondary reaction hypothesis. It should be noted that this hypothesis is purely speculative, as neither the rate of the $CF_2Cl + CH_3$ reaction nor the exact values of Cl atom concentrations used in ref 30 are known.

The results of the current study are in agreement with those of the earlier low-temperature investigations (Figure 4). Of these earlier studies, those of Whytock et al.[23] and Zahniser et al.[26] covered the largest temperature interval, 200−500 K. If the temperature dependence of k_1 obtained in the current work is combined with the values of ref 23, then the resultant combined set of data can be represented with the following modified Arrhenius expression:

$$k_1 = 5.69 \times 10^{-19} T^{2.49} \exp(-609\ \mathrm{K}/T)\ \mathrm{cm^3\ molecule^{-1}\ s^{-1}} \quad (200-1104\ \mathrm{K}) \quad \text{(IX)}$$

The maximum deviation of the experimental rate constant values from expression IX is 11.4%.

The Cl atom has a low-lying excited spin−orbit state ($^2P_{1/2}$, 10.5 kJ mol^{-1} relative to the ground $^2P_{3/2}$ state). A difference in reactivity in these two electronic states toward CH_4 was suggested by Ravishankara and Wine as a potential factor affecting the values of k_1 obtained by different experimental techniques. The issue of spin−orbit quenching was extensively discussed by Wang and Keyser,[18] who used large concentrations of an efficient quencher (CF_4) in their discharge flow/resonance fluorescence experiments and demonstrated that nonequilibration of spin−orbit states had no effect on the rate constant of reaction 1. In the current work, even larger concentrations of CF_4 were used (Table 1), and thus, considering the efficiency of CF_4 as a spin−orbit quencher (quenching rate constant in the $(0.23-1.5) \times 10^{-10}$ cm^3 $molecule^{-1}$ s^{-1} range[58−60]), the values of k_1 obtained should represent the reaction of completely spin−orbit equilibrated Cl atoms. It is also worth noting that a recent experimental study by Kim et al.[72] demonstrated very low reactivity of the excited $Cl(^2P_{1/2})$ state toward CH_4.

Reaction $Cl + CH_3Cl \rightarrow HCl + CH_2Cl$ (2). Figure 5 presents the results of direct studies of reaction 2 and those of indirect studies where temperature dependences were reported. Clyne and Walker[17] obtained the $k_1(T)$ dependence in the 300−604 K temperature interval by the discharge flow/mass spectrometry method. Manning and Kurylo[22] studied reaction 2 at low temperatures (233−322 K) by the flash photolysis/resonance fluorescence technique. Tshuikow-Roux et al.[38] and Orlando[46] obtained temperature dependences of k_2 using the relative-rates technique. The $Cl + C_2H_5Cl$ reaction was used as a reference reaction in ref 38, and in ref 46, the $Cl + CH_4$ (1) and the $Cl + CH_3Br$ reactions were used as references. Figure 5 presents the data of Orlando obtained relative to the well-studied reaction 1; the $k_1(T)$ dependence of Whytock et al. was used (in the current work) to convert the k_2/k_1 values[46] to those of k_2.

The results of the current study are in agreement with the low-temperature $k_2(T)$ dependences of refs 22, 38, and 46 and with the room-temperature values of k_2 obtained in the relative-rate studies of refs 39, 40, and 42 (listed in the caption to Figure 5). Above ambient temperature, the k_2 values of Clyne and Walker are significantly larger than the results of the current work. Similar differences between the results of ref 17 and other studies were observed for reactions 1, 3, and 4 (see also the discussion of ref 17 above in relation to the $Cl + CH_4$ reaction). At low temperatures, the minor differences between the values

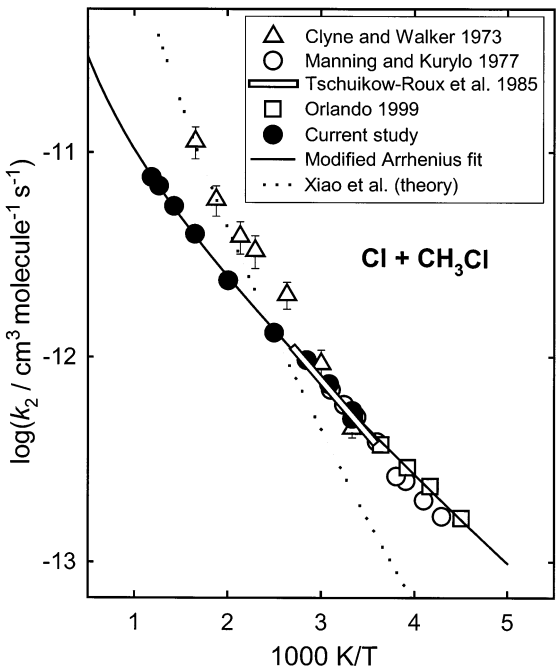

Figure 5. Temperature dependence of the rate constant of reaction 2. Results of direct studies and indirect studies where temperature dependences were reported are displayed: Clyne and Walker,[17] Manning and Kurylo,[22] Tschuikow-Roux et al.,[38] Orlando,[46] and the current study. Here, the relative-rate data of ref 46 (k_2/k_1, 222−298 K) were converted to the values of k_2 using the experimental $k_1(T)$ dependence of Whytock et al.[23] Results of three room-temperature relative-rate studies (4.6×10^{-13},[40] 5.3×10^{-13},[39] and 5.1×10^{-13} [42] if the results of the current study are used for the rate constants of the reference reactions) are in general agreement with the results of the current work and are not displayed to avoid plot congestion. The thin solid line represents the modified Arrhenius fit of eq VI. The dotted line shows the $k_2(T)$ dependence obtained in the theoretical study of Xiao et al.[87]

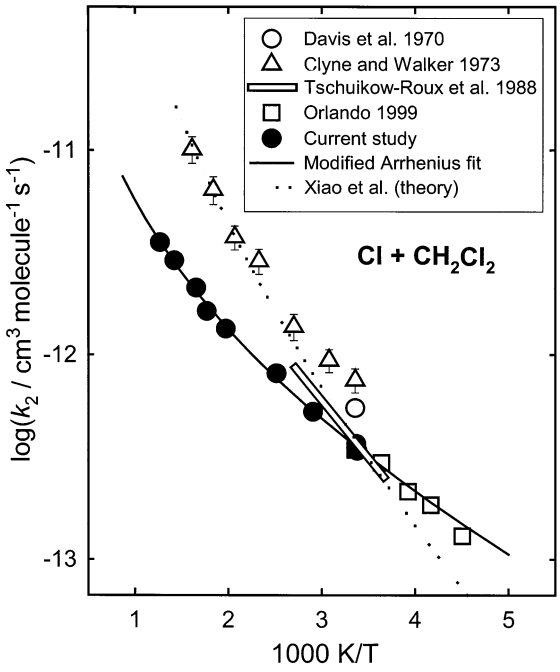

Figure 6. Temperature dependence of the rate constant of reaction 3. Results of direct studies and indirect studies where temperature dependences were reported are displayed: Davis et al.,[36] Clyne and Walker,[17] Tschuikow-Roux et al.,[37] Orlando,[46] and the current study. Rate constant values reported in three room-temperature relative-rate studies (4.0×10^{-13},[40] 3.9×10^{-13},[41] and 3.8×10^{-13} [42] if the results of the current study are used for the rate constants of the reference reactions) are approximately 10% larger than the results of the current work and are not displayed to avoid plot congestion. The thin solid line represents the modified Arrhenius fit of eq VII. The dotted line shows the $k_3(T)$ dependence obtained in the theoretical study of Xiao et al.[86]

of k_2 derived from the k_2/k_1 values of Orlando and the $k_2(T)$ dependence of Manning and Kurylo disappear if the data of Orlando are used with the $k_1(T) = 1.1 \times 10^{-11} \exp(-1400\ \mathrm{K}/T)$ $\mathrm{cm^3\ molecule^{-1}\ s^{-1}}$ dependence recommended in ref 31 (as was done in ref 46) instead of the $k_1(T)$ dependence of Whytock et al.[23]

Reaction Cl + CH_2Cl_2 → HCl + $CHCl_2$ (3). Figure 6 presents the results of the direct studies of reaction 3 and those of the indirect studies where temperature dependences were reported. Displayed are the results of Davis et al.[36] (flash photolysis/resonance fluorescence), Clyne and Walker[17] (discharge flow/mass spectrometry), Tschuikow-Roux et al.[37] (relative rates, reaction 1 used as a reference reaction), and Orlando[46] (relative rates, reactions 1 and Cl + CH_3Br used as reference reactions). Figure 6 presents the data of Orlando obtained relative to the well-studied reaction 1; the $k_1(T)$ dependence of Whytock et al. was used (in the current work) to convert the k_3/k_1 values[46] to those of k_3.

The results of the current study are in agreement with the lower-temperature $k_3(T)$ dependence derived from the relative-rate measurements of Orlando. The $k_3(T)$ dependence derived from the relative-rates study of Tschuikow-Roux et al. shows a larger activation energy although the room-temperature value coincides with that of the current work. The room-temperature relative-rate determinations of refs 40−42 provide k_3 values (listed in the caption to Figure 6 but not displayed to avoid plot congestion) that are approximately 10% larger than those obtained in the current work. The value of Davis et al.[36] is 55% larger than the current results; the room-temperature rate constant of reaction 1 reported in the same work (1.5×10^{-13} $\mathrm{cm^3\ molecule^{-1}\ s^{-1}}$) is also larger than those reported in other direct studies by ∼40−50%, indicating potential systematic factors affecting these experiments. The k_3 values of Clyne and Walker[17] are, on average, a factor of 3 larger than those of the current work, also in disagreement with the low-temperature data.[40−42,46]

Reaction Cl + $CHCl_3$ → HCl + CCl_3 (4). Figure 7 presents the results of the direct studies of reaction 4 and those of the indirect studies where temperature dependences were reported: Clyne and Walker[17] (discharge flow/mass spectrometry), Talhaoui et al.[45] (discharge flow/mass spectrometry), Orlando[46] (relative rates, reactions 1 and Cl + CH_3Br used as reference reactions), and the current study. Figure 7 presents the data of Orlando obtained relative to the well-studied reaction 1; the $k_1(T)$ dependence of Whytock et al. was used (in the current work) to convert the k_4/k_1 values[46] to those of k_4. Also displayed is the room-temperature determination of Jeoung et al.,[43] who used the very-low-pressure reactor technique with mass spectrometry and chemiluminescence as detection methods to study the N + $CHCl_3$ reaction. As a part of that investigation, they obtained a value of $k_4 = (3.7 \pm 1.0) \times 10^{-14}$ $\mathrm{cm^3\ molecule^{-1}\ s^{-1}}$ that is at least a factor of 2 lower than the rest of the literature data included in Figure 7 and its caption.

References 17 and 45 used very similar direct experimental techniques with Cl atoms in large excess over $CHCl_3$ and with mass spectrometric detection of the reactants. Nevertheless, the values of k_4 reported by Clyne and Walker[17] are significantly larger than those of Talhaoui et al.,[45] which are in agreement with the results of the current study. This situation is similar to

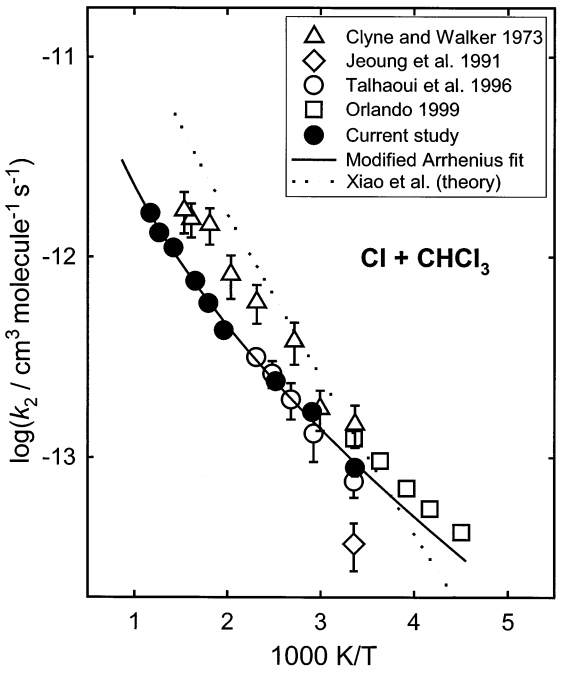

Figure 7. Temperature dependence of the rate constant of reaction 4. Results of direct studies and indirect studies where temperature dependences were reported are displayed: Clyne and Walker,[17] Talhaoui et al.,[45] Orlando,[46] and the current study. Rate constant values reported in three room-temperature relative-rate studies (not displayed to avoid plot congestion: 1.25×10^{-13},[42] 1.20×10^{-13},[41] and 1.39×10^{-13} [44] if the results of the current study are used for the rate constants of the reference reactions) are 30−50% larger than the results of the current work and are in agreement with the relative-rate values of Orlando. Also displayed is the value of Jeoung et al.[43] obtained by the very-low-pressure reactor technique. The thin solid line represents the modified Arrhenius fit of eq VIII. The dotted line shows the $k_4(T)$ dependence obtained in the theoretical study of Xiao et al.[86]

what is observed for other reactions investigated in this work and in ref 17: the values of rate constants determined in ref 17 are larger than those obtained later by similar or different techniques (see the discussion of reaction 1).

The results of the relative-rate studies (room-temperature investigations of refs 41, 42, and 44—see the caption to Figure 7—and the temperature-dependent study of ref 46) are in agreement with each other. However, the rate constant values resulting from these relative-rate studies ($k_4(298\ \text{K}) = (1.2-1.4) \times 10^{-13}$ cm^3 molecule^{-1} s^{-1}) are systematically larger than those of the direct investigations ($k_4(298\ \text{K}) = (7.6 \pm 1.3) \times 10^{-14}$ cm^3 molecule^{-1} s^{-1} reported by Talhaoui et al.[45] and $k_4(297\ \text{K}) = (8.9 \pm 1.6) \times 10^{-14}$ cm^3 molecule^{-1} s^{-1} obtained in the current work, systematic contributions are included in the value of the uncertainty). The differences, however, are comparable to the uncertainties reported in the individual studies. Part of the uncertainty associated with the relative-rate studies is due to the uncertainties in the rate constants of the reference reactions. For example, if the $k_1(T) = 1.1 \times 10^{-11} \exp(-1400\ \text{K}/T)$ cm^3 molecule^{-1} s^{-1} dependence recommended in ref 31 is used together with the k_4/k_1 values of ref 46 instead of the $k_1(T)$ dependence of Whytock et al.,[23] then the room-temperature value of k_4 is reduced from 1.25×10^{-13} to 1.15×10^{-13} cm^3 molecule^{-1} s^{-1}. The latter value, considering the reported[46] ±10% uncertainty in the k_4/k_1 ratio, agrees with the results of the current study within the combined uncertainties of both works.

III.2. Theoretical Studies of Reactions 1−4. The reaction of Cl atoms with CH_4 has been the subject of numerous theoretical studies. Reviews of relevant literature can be found, for example, in refs 32, 33, 73, and 74. A number of studies concentrated on applying different versions of transition-state theory to either fit the experimental $k_1(T)$ dependence (e.g., refs 73 and 75) or predict it from basic principles (e.g., ref 74 and references therein). A different approach was undertaken by Michelsen and Simpson.[32,33,76] These authors analyzed a large variety of information on reaction 1, including experimental and theoretical studies of its rates, kinetic isotope effects, and mode-specific dynamics, and created a reaction model based on both thermal kinetic data and data on the enhancement of the reaction rate by vibrational excitation of certain modes of CH_4. This model was used to reproduce the $k_1(T)$ dependence including non-Arrhenius curvature and to extrapolate the experimental data to extreme conditions.

Another distinctly different approach to the theoretical analysis of the kinetics of reaction 1 was presented recently by Donahue,[66] who analyzed reactivity trends in a series of atom transfer reactions on the basis of the interaction of ground and ionic states along the reaction coordinate. This work offered a formalism of the theoretical interpretation of the experimental data that enables a factoring out of contributions of individual phenomena such as tunneling and thermal vibrational excitation of certain, most critical, transitional modes.

In one of the latest computational studies, Corchado et al. [73] applied variational transition-state theory with multidimensional semiclassical tunneling transmission coefficients to calculate the $k_1(T)$ temperature dependence. These authors used an analytical potential energy surface based on quantum chemical calculations and calibrated against the experimental room-temperature value of k_1. The resultant calculated values of k_1 (dotted line in Figure 4, the "CUS/μOMT" model of ref 73) coincide with the experimental data at temperatures up to 800 K, where the calculated $k_1(T)$ dependence displays a discontinuity in its derivative, as reflected by the broken dotted line in Figure 4. The calculated k_1 values at $T > 800$ K are, as a result, lower than the experimental results. This nonphysical phenomenon that can be attributed only to an artifact of the computational method unfortunately prevents the potential use of the model of Corchado et al. for extrapolation of the experimental $k_1(T)$ dependence to higher temperatures, despite the excellent agreement of the computed and experimental k_1 values at $T < 800$ K.

To provide for such an extrapolation, a transition-state theory model of reaction 1 was created in the current work. An initial approximation to the properties of the reaction transition state (geometry and vibrational frequencies) was obtained in ab initio calculations using the UMP2/6-311G(2d,2p) method. Rate constant values were calculated using the classical transition-state theory formula (see, for example, ref 77). Ab initio calculations at the level used here cannot be expected to yield an exact value of the energy barrier. Similarly, properties of the transition state that determine the preexponential factor generally are not accurately predicted by such medium-level quantum chemical calculations. In particular, frequencies of the bending modes of the Cl−H−CH_3 transitional structure are especially susceptible to error because of their coupling to the energy barrier.[66] Thus, to reproduce the experimental temperature dependence of the rate constant, an adjustment of the lowest double-degenerate vibrational frequency of the bending mode of the transition state and of the reaction barrier height was performed. A combined set of data formed by the results of the current study and by those of Whytock et al.[23] (included to represent the low-temperature $k_1(T)$ dependence) was used in the fitting. A quantum tunneling correction was computed

TABLE 2: Properties of the Transition State Theory Model of Reaction 1

transition state	
vibrational frequencies (cm^{-1}) and degeneracies	510[a] [385] (2), 516, 958 (2), 1208, 1460 (2), 3136, 3304 (2)
rotational constant, symmetry number, and dimension	0.5641, 3, 3
CH_4, HCl, and CH_3	Molecular properties were taken from ref 93.
Cl	Properties were taken from ref 93. The existence of the excited spin−orbit level (882.5 cm^{-1}, degeneracy 2) is taken into account when computing the electronic partition function.
direct reaction barrier	14.27 kJ mol^{-1}
reverse reaction barrier	9.76 kJ mol^{-1}
barrier width[b]	$l = 0.829$ $amu^{1/2}$ Å

[a] This value was adjusted in the data-fitting process. The original value obtained in ab initio calculations is given in square brackets. All other frequencies were obtained in UMP2/6-311G(2d,2p) level ab initio calculations. [b] Obtained from UMP2/6-311G(2d,2p) level IRC[80,81] calculations. This value of the barrier width results in the 973i cm^{-1} value of the imaginary frequency. References 15, 16, 78, and 79 can be consulted for details of the methodology.

using the "barrier width" method.[15,78,79] The shape of the reaction potential energy barrier was determined using the method of the reaction path following (intrinsic reaction coordinate, IRC)[80,81] in mass-weighted internal coordinates. The resultant barrier potential energy profiles were fitted with the unsymmetrical Eckart function[82] to determine the width parameter l that was used in the calculation of the tunneling correction. Details of the computational approach can be found in refs 15 and 16. Parameters of the model are given in Table 2.

The resultant model reproduces the experimental $k_1(T)$ dependence very well (Figure 4). The rate constant values extrapolated via modeling can be represented by the modified Arrhenius expression

$$k_1 = 5.26 \times 10^{-19}\, T^{2.49} \exp(-589\ \mathrm{K}/T)\ \mathrm{cm^3\ molecule^{-1}\ s^{-1}} \quad (200-3000\ \mathrm{K}) \quad \text{(X)}$$

with deviations from the calculated values of less than 6% between 200 and 2000 K and the largest deviation of 19% at 3000 K. It should be noted that expression IX also provides an adequate representation of the modeled $k_1(T)$ dependence below 2000 K with deviations of less than 9% (although a larger deviation of 28% is observed at 3000 K). Temperature-specific values of the deviations of eqs IX and X from the $k_1(T)$ dependence of the model are given in Supporting Information (Table 2S).

In 1994, Rayez et al.[83] studied reactions 2−4 by performing the quantum chemical calculations (HF/6-31G(d,p) geometry optimization and frequencies with BAC-MP4[84,85] energy calculations) and computing the rate constants using Eckart tunneling corrections. These authors did not publish the complete temperature dependences of the rate constants, reporting only the room-temperature values. These calculated room-temperature values of k_2 and k_3 were factors of 8.3 and 2.7, respectively, less than the experimental ones; the calculated k_4 value was larger than the experimental one by a factor of 2.7.

Recently, Xiao et al.[86,87] performed computational modeling of reactions 2−4 using variational transitional-state theory with a "small-curvature" semiclassical tunneling correction. For each reaction, the minimum-energy path was optimized at the BH&HLYP/6-311G(d,p) level, and vibrational frequencies were obtained at the same level of theory. The energy along the reaction path was refined at the QCISD(T)/6-311+G(d,p) level. References 88−91 can be consulted for the details of the these computational methods. The resultant values of the rate constants are shown in Figures 5−7 by the dotted lines. As can be seen from the plots, the calculated values are in disagreement with experiment, with both preexponential factors and activation energies exceeding the experimental values. The differences between the calculated and the experimental data are not surprising since generally one cannot expect preexponential factors and reaction barriers to be reproduced with chemical accuracy at the computational levels used. Despite the failure of these calculations to reproduce the experiment quantitatively, qualitative findings are useful for the further modeling of reactions 2−4. It was demonstrated in refs 86 and 87 that in reactions 2−4 the contribution of the zero-point vibrational energy (ZPE) to the potential energy profile along the reaction path is quite substantial (i.e., the dependence of the ZPE on the reaction coordinate significantly affects how the total (vibrationally adiabatic) potential energy given by the sum of the electronic energy and ZPE changes along the reaction path). In particular, as can be seen from the plots presented in refs 86 and 87, the widths of the potential energy barriers of reactions 2−4 are significantly different (larger) if the ZPE is included compared to the widths obtained if only the electronic energy is taken into account. One consequence of this effect is that models of reactions 2−4 created in a manner similar to that used in the current study for reaction 1 would overestimate the contribution of tunneling if the barrier-width values are obtained on the basis of IRC following without the contribution of ZPE taken into account. Moreover, the modeling of reaction 4 performed in refs 86 and 87 demonstrates noticeable variational effects: calculations where the position of the transition state was chosen by minimizing the reactive flux at each temperature (canonical variational approach) resulted in rate constant values that are different from those obtained using the simpler nonvariational version of the transition-state theory by approximately a factor of 5 at room temperature.

The level of calculations used by the authors of refs 86 and 87 to evaluate vibrational frequencies results in entropic (preexponential) factors that are significantly larger than the experimental results. This casts doubts on the reliability of the ZPE versus reaction coordinate dependences and the resultant shapes of the vibrationally adiabatic potential energy profiles. Reliable evaluation of the shapes (and widths) of the reaction barriers would require careful studies using a variety of different computational methods to ensure that the results are not artifacts. Considering the above effects of the ZPE on the barrier widths of reactions 2−4 and the variational effects observed in reaction 4, we chose not to perform transition-state theory-based modeling of these reactions in the current work. Although such modeling is desirable for the extrapolation of the experimental data, the complications of accounting for ZPE variations along the reaction path put such a task beyond the scope of this experimental study.

It should be noted that, on the basis of the computational results of refs 73 and 74, a similar effect of the ZPE versus reaction coordinate dependence on the shape and width of the

vibrationally adiabatic energy profile along the reaction path can potentially be expected for reaction 1. Nevertheless, the transition-state theory model of reaction 1 created in the current work using the barrier width evaluated on the basis of only the electronic energy profile (without ZPE) reproduces the experimental data, including the curvature of the Arrhenius plot, very well (Figure 4). A similar approach applied to reaction 2 fails: a transition-state theory model with parameters fitted to reproduce the experiment results in the curvature of the $\ln(k_2)$ versus T^{-1} dependence that is much larger than the experimental one. In this modeling attempt performed in the current work, the UMP2/6-311G(2d,2p)-based barrier width of $l = 1.02$ amu$^{1/2}$ Å was used for reaction 2 (see refs 15, 78, and 79 for the meaning of the barrier width parameter). The good results of modeling obtained for reaction 1 may be due to a fortuitous cancellation of errors where the overestimation of tunneling due to the underestimated barrier width is compensated, to some extent, by the lack of accounting for reaction path curvature and resultant "corner-cutting" tunneling. Comparison of the tunneling correction factors obtained with the model of reaction 1 created in the current study with those calculated using semiclassical multidimensional tunneling on the ZPE-corrected vibrationally adiabatic potential energy surface[73,74] reveals similar values: 6.2/12.8/4.3 at 200 K, 2.5/3.3/2.0 at 300 K, 1.7/2.0/1.6 at 400 K, and 1.3/1.4/1.2 at 600 K. Here, the values of the tunneling correction factors are presented as (current study)/(ref 73)/(ref 74). As can be seen, the differences between the results of multidimensional tunneling calculations performed using similar methods but different details of the potential energy surface are larger than those between each of these models and the one-dimensional model of the current study.

III.3. Rate Constants of the Reverse R + HCl → Cl + RH Reactions. Information on reactions 1−4 obtained in the current work can be used in combination with the known thermochemistry of these reactions to derive the temperature dependences of the rate constants of the reverse processes, those of the reactions of methyl and chlorinated methyl radicals with HCl:

$$CH_3 + HCl \rightarrow Cl + CH_4 \qquad (-1)$$

$$CH_2Cl + HCl \rightarrow Cl + CH_3Cl \qquad (-2)$$

$$CHCl_2 + HCl \rightarrow Cl + CH_2Cl_2 \qquad (-3)$$

$$CCl_3 + HCl \rightarrow Cl + CHCl_3 \qquad (-4)$$

The transition-state theory model of reaction 1 (see preceding subsection) created in the current study results in the $k_{-1}(T)$ dependence, which can be represented with the expression

$$k_{-1} = 5.48 \times 10^{-20} T^{2.27} \exp(253\ \mathrm{K}/T)\ \mathrm{cm^3\ molecule^{-1}\ s^{-1}} \quad (200-3000\ \mathrm{K}) \quad \text{(XI)}$$

The experimental rate constant values of reactions 2−4 converted into those of the reverse reactions result in the following Arrhenius expressions within the corresponding experimental temperature intervals (shown in parentheses):

$$k_{-2} = 2.64 \times 10^{-13} \exp(-2828\ \mathrm{K}/T)\ \mathrm{cm^3\ molecule^{-1}\ s^{-1}} \quad (300-843\ \mathrm{K}) \quad \text{(XII)}$$

$$k_{-3} = 2.08 \times 10^{-13} \exp(-4551\ \mathrm{K}/T)\ \mathrm{cm^3\ molecule^{-1}\ s^{-1}} \quad (296-790\ \mathrm{K}) \quad \text{(XIII)}$$

$$k_{-4} = 1.56 \times 10^{-13} \exp(-6019\ \mathrm{K}/T)\ \mathrm{cm^3\ molecule^{-1}\ s^{-1}} \quad (297-854\ \mathrm{K}) \quad \text{(XIV)}$$

Here, thermochemical properties from refs 92−101 were used. Reference 15 can be consulted for the details of the thermochemical models of the individual species involved. The uncertainties in expressions XI−XIV originate primarily from those in the enthalpies of reactions 1−4. These uncertainty factors can be calculated for any temperature using the van't Hoff factor with the following cumulative reaction enthalpy uncertainties: 1.9, 3.9, 3.5, and 3.8 kJ mol^{-1} for reactions 1, 2, 3, and 4, respectively.

The temperature dependence of the rate constant of reaction −1 given by expression XI is in general agreement with the experimental values of Russell et al.[102] and gives a room-temperature value of k_{-1} that is 25% lower than that of Dobis and Benson.[28] The approximate agreement is not surprising since the value of $\Delta H^{\circ}_{f298}(CH_3)$ used in the calculations is in agreement with those derived from refs 28 and 102. No experimental information is available on reactions −2, −3, and −4.

IV. Conclusions

Reactions of Cl atoms with methane and three chlorinated methanes have been studied experimentally with the discharge flow/resonance fluorescence technique over wide ranges of temperatures and at pressures between 1.4 and 8.8 Torr. The resultant rate constants can be represented with the modified Arrhenius expressions V−VIII. The rate constants k_1 of the reaction of Cl atoms with methane obtained in the current study agree with the results of earlier low-temperature measurements. Combination of the temperature dependence of k_1 obtained in the current work at temperatures ranging from ambient to 1104 K with the low-temperature literature data (represented by ref 23) results in the $k_1(T)$ dependence described by eq IX. Extrapolation of the experimental data of reaction 1 to higher temperatures via a transition-state model results in a $k_1(T)$ dependence that can also be well represented by eq IX or, with slightly better accuracy, by eq X.

It is demonstrated that the existing theoretical models of reactions 2−4 are in disagreement with the experiments and thus are not suitable for use in extrapolating the experimental results to conditions outside the experimental ranges. Thus, no better alternative to the use of the experimental fits of eqs VI−VIII can be proposed at this time. The temperature dependences of the rate constants of reactions 1−4 combined with the known thermochemistry of these reactions result in the temperature dependences of the reverse R + HCl → Cl + RH reactions given by eqs XI−XIV.

Acknowledgment. This research was supported by the National Science Foundation, Combustion and Thermal Plasmas Program under grant no. CTS-9807136. We thank Dr. L. J. Stief for helpful advice and the loan of equipment, Dr. V. L. Orkin for advice and help with the analyses of chloromethane samples, and Mr. E. V. Shafir for help with the analyses of chloromethane samples.

Supporting Information Available: Results of the ab initio calculations of the transition state of reaction 1 (Table 1S), calculated values of the rate constants of reactions 1 and −1 as a function of temperature (Table 2S), and a comparison of the calculated and the literature data on the rate constants of reaction −1 (Figure 1S). This material is available free of charge via the Internet at http://pubs.acs.org.

References and Notes

(1) Karra, S. B.; Gutman, D.; Senkan, S. M. *Combust. Sci. Technol.* **1988**, *60*, 45.

(2) Chang, W. D.; Senkan, S. M. *Environ. Sci. Technol.* **1989**, *23*, 442.
(3) Lee, K. Y.; Yang, M. H.; Puri, I. K. *Combust. Flame* **1993**, *92*, 419.
(4) Wang, H.; Hahn, T. O.; Sung, C. J.; Law, C. K. *Combust. Flame* **1996**, *105*, 291.
(5) Chang, W. D.; Karra, S. B.; Senkan, S. M. *Combust. Sci. Technol.* **1986**, *49*, 107.
(6) Karra, S. B.; Senkan, S. M. *Combust. Sci. Technol.* **1987**, *54*, 333.
(7) Xieqi, M.; Cicek, B.; Senkan, S. M. *Combust. Flame* **1993**, *94*, 131.
(8) Cicek, B.; Senkan, S. M. *Combust. Sci. Technol.* **1993**, *91*, 53.
(9) Cui, J. P.; He, Y. Z.; Tsang, W. *J. Phys. Chem.* **1989**, *93*, 724.
(10) Lee, K. Y.; Puri, I. K. *Combust. Flame* **1993**, *92*, 440.
(11) Lee, K. Y.; Puri, I. K. *Combust. Flame* **1993**, *94*, 191.
(12) Taylor, P. H.; Tirey, D. A.; Dellinger, B. *Combust. Flame* **1996**, *104*, 260.
(13) Taylor, P. H.; Tirey, D. A.; Dellinger, B. *Combust. Flame* **1996**, *106*, 1.
(14) Ho, W. P.; Yu, Q.-R.; Bozzelli, J. W. *Combust. Sci. Technol.* **1992**, *85*, 23.
(15) Bryukov, M. G.; Slagle, I. R.; Knyazev, V. D. *J. Phys. Chem. A* **2001**, *105*, 3107.
(16) Bryukov, M. G.; Slagle, I. R.; Knyazev, V. D. *J. Phys. Chem. A* **2001**, *105*, 6900.
(17) Clyne, M. A. A.; Walker, R. F. *J. Chem. Soc., Faraday Trans. 1* **1973**, *69*, 1547.
(18) Wang, J. J.; Keyser, L. F. *J. Phys. Chem. A* **1999**, *103*, 7460.
(19) Watson, R.; Machado, G.; Fischer, S.; Davis, D. D. *J. Chem. Phys.* **1976**, *65*, 2126.
(20) Keyser, L. F. *J. Chem. Phys.* **1978**, *69*, 214.
(21) Poulet, G.; Le Bras, G.; Combourieu, J. *J. Chim. Phys.* **1974**, *71*, 101.
(22) Manning, R. G.; Kurylo, M. J. *J. Phys. Chem.* **1977**, *81*, 291.
(23) Whytock, D. A.; Lee, J. H.; Michael, J. V.; Payne, W. A.; Stief, L. J. *J. Chem. Phys.* **1977**, *66*, 2690.
(24) Baghal-Vayjooee, M. H.; Colussi, A. J.; Benson, S. W. *J. Am. Chem. Soc.* **1978**, *100*, 3214.
(25) Lin, C. L.; Leu, M. T.; DeMore, W. B. *J. Phys. Chem.* **1978**, *82*, 1772.
(26) Zahniser, M. S.; Berquist, B. M.; Kaufman, F. *Int. J. Chem. Kinet.* **1978**, *10*, 15.
(27) Ravishankara, A. R.; Wine, P. H. *J. Chem. Phys.* **1980**, *72*, 25.
(28) Dobis, O.; Benson, S. W. *Int. J. Chem. Kinet.* **1987**, *19*, 691.
(29) Seeley, J. V.; Jayne, J. T.; Molina, M. J. *J. Phys. Chem.* **1996**, *100*, 4019.
(30) Pilgrim, J. S.; McIlroy, A.; Taatjes, C. A. *J. Phys. Chem. A* **1997**, *101*, 1873.
(31) DeMore, W. B.; Sander, S. P.; Golden, D. M.; Hampson, R. F.; Kurylo, M. J.; Howard, C. J.; Ravishankara, A. R.; Kolb, C. E.; Molina, M. J. *JPL Publ.* **1997**, *97*−*4*.
(32) Michelsen, H. A. *Acc. Chem. Res.* **2001**, *34*, 331.
(33) Michelsen, H. A.; Simpson, W. R. *J. Phys. Chem. A* **2001**, *105*, 1476.
(34) Atkinson, R.; Baulch, D. L.; Cox, R. A.; Hampson, R. F., Jr.; Kerr, J. A.; Rossi, M. J.; Troe, J. *J. Phys. Chem. Ref. Data* **1997**, *26*, 521.
(35) Knox, J. H. *Trans. Faraday Soc.* **1962**, *58*, 275.
(36) Davis, D. D.; Braun, W.; Bass, A. M. *Int. J. Chem. Kinet.* **1970**, *2*, 101.
(37) Tschuikow-Roux, E.; Faraji, F.; Paddison, S.; Niedzielski, J.; Miyokawa, K. *J. Phys. Chem.* **1988**, *92*, 1488.
(38) Tschuikow-Roux, E.; Yano, T.; Niedzielski, J. *J. Chem. Phys.* **1985**, *82*, 65.
(39) Wallington, T. J.; Andino, J. M.; Ball, J. C.; Japar, S. M. *J. Atmos. Chem.* **1990**, *10*, 301.
(40) Niki, H.; Maker, P. D.; Savage, C. M.; Breitenbach, L. P. *Int. J. Chem. Kinet.* **1980**, *12*, 1001.
(41) Catoire, V.; Lesclaux, R.; Schneider, W. F.; Wallington, T. J. *J. Phys. Chem.* **1996**, *100*, 14356.
(42) Beichert, P.; Wingen, L.; Lee, J.; Vogt, R.; Ezell, M. J.; Ragains, M.; Neavyn, R.; Finlayson-Pitts, B. J. *J. Phys. Chem.* **1995**, *99*, 13156.
(43) Jeoung, S. C.; Choo, K. Y.; Benson, S. W. *J. Phys. Chem.* **1991**, *95*, 7282.
(44) Brahan, K. M.; Hewitt, A. D.; Boone, G. D.; Hewitt, S. A. *Int. J. Chem. Kinet.* **1996**, *28*, 397.
(45) Talhaoui, A.; Louis, F.; Meriaux, B.; Devolder, P.; Sawerysyn, J.-P. *J. Phys. Chem.* **1996**, *100*, 2107.
(46) Orlando, J. J. *Int. J. Chem. Kinet.* **1999**, *31*, 515.
(47) Kaufman, F. *Prog. React. Kinet.* **1961**, *1*, 1.
(48) Poirier, R. V.; Carr, R. W. *J. Phys. Chem.* **1971**, *75*, 1593.
(49) Howard, C. J. *J. Phys. Chem.* **1979**, *83*, 3.
(50) Ogren, P. J. *J. Phys. Chem.* **1975**, *79*, 1749.
(51) Sepehrad, A.; Marshall, R. M.; Purnell, H. *Int. J. Chem. Kinet.* **1979**, *11*, 411.
(52) Ogryzlo, E. A. *Can. J. Chem.* **1961**, *39*, 2556.
(53) Davis, D. D.; Braun, W. *Appl. Opt.* **1968**, *7*, 2071.
(54) Okabe, H. *Photochemistry of Small Molecules;* Wiley: New York, 1978.
(55) Stickel, R. E.; Nicovich, J. M.; Wang, S.; Zhao, Z.; Wine, P. H. *J. Phys. Chem.* **1992**, *96*, 9875.
(56) Bedjanian, Y.; Laverdet, G.; Le Bras, G. *J. Phys. Chem. A* **1998**, *102*, 953.
(57) Nicovich, J. M.; Wine, P. H. *Int. J. Chem. Kinet.* **1990**, *22*, 379.
(58) Clark, R. H.; Husain, D. *J. Photochem.* **1983**, *21*, 93.
(59) Chichinin, A. I.; Krasnoperov, L. N. *Chem. Phys. Lett.* **1989**, *160*, 448.
(60) Tyndall, G. S.; Orlando, J. J.; Kegley-Owen, C. S. *J. Chem. Soc., Faraday Trans.* **1995**, *91*, 3055.
(61) Lambert, M.; Sadowski, C. M.; Carrington, T. *Int. J. Chem. Kinet.* **1985**, *17*, 685.
(62) *Chemical Engineer's Handbook*, 5th ed.; Perry, R. H., Chilton, C. H. E., Eds.; McGraw-Hill: New York, 1973.
(63) Timonen, R. S.; Gutman, D. *J. Phys. Chem.* **1986**, *90*, 2987.
(64) Seetula, J. A.; Gutman, D.; Lightfoot, P. D.; Rayes, M. T.; Senkan, S. M. *J. Phys. Chem.* **1991**, *95*, 10688.
(65) Timonen, R. S.; Russell, J. J.; Gutman, D. *Int. J. Chem. Kinet.* **1986**, *18*, 1193.
(66) Donahue, N. M. *J. Phys. Chem. A* **2001**, *105*, 1489.
(67) Wallington, T. J.; Skewes, L. M.; Siegl, W. O.; Wu, C.-H.; Japar, S. M. *Int. J. Chem. Kinet.* **1988**, *20*, 867.
(68) Atkinson, R.; Aschmann, S. M. *Int. J. Chem. Kinet.* **1985**, *17*, 33.
(69) Rowley, D. M.; Lesclaux, R.; Lightfoot, P. D.; Noziere, B.; Wallingotn, T. J.; Hurley, M. D. *J. Phys. Chem.* **1992**, *96*, 4889.
(70) Taatjes, C. A. Private communication.
(71) Jones, Y.; Holmes, B. E.; Duke, D. W.; Tipton, D. L. *J. Phys. Chem.* **1990**, *94*, 4957.
(72) Kim, Z. H.; Alexander, A. J.; Bechtel, H. A.; Zare, R. N. *J. Chem. Phys.* **2001**, *115*, 179.
(73) Corchado, J. C.; Truhlar, D. G.; Espinosa-Garcia, J. *J. Chem. Phys.* **2000**, *112*, 9375.
(74) Roberto-Neto, O.; Coitino, E. L.; Truhlar, D. G. *J. Phys. Chem. A* **1998**, *102*, 4568.
(75) Furue, H.; Pacey, P. D. *J. Phys. Chem.* **1990**, *94*, 1419.
(76) Michelsen, H. A. *J. Geophys. Res., [Atmos.]* **2001**, *106*, 12267.
(77) Johnston, H. S. *Gas-Phase Reaction Rate Theory*; The Ronald Press: New York, 1966.
(78) Knyazev, V. D.; Bencsura, A.; Stoliarov, S. I.; Slagle, I. R. *J. Phys. Chem.* **1996**, *100*, 11346.
(79) Knyazev, V. D.; Slagle, I. R. *J. Phys. Chem.* **1996**, *100*, 16899.
(80) Fukui, K. *Acc. Chem. Res.* **1981**, *14*, 363.
(81) Gonzalez, C.; Schlegel, H. B. *J. Phys. Chem.* **1990**, *94*, 5523.
(82) Eckart, C. *Phys. Rev.* **1930**, *35*, 1303.
(83) Rayez, M.-T.; Rayez, J.-C.; Sawerysyn, J.-P. *J. Phys. Chem.* **1994**, *98*, 11342.
(84) Ho, P.; Melius, C. F. *J. Phys. Chem.* **1990**, *94*, 5120.
(85) Melius, C. F.; Binkley, J. S. *Symp. (Int.) Combust., [Proc.]* **1984**, *20*, 575.
(86) Xiao, J. F.; Li, Z. S.; Ding, Y. H.; Liu, J. Y.; Huang, X. R.; Sun, C. C. *J. Phys. Chem. A* **2002**, *106*, 320.
(87) Xiao, J. F.; Li, Z. S.; Ding, Y. H.; Liu, J. Y.; Huang, X. R.; Sun, C. C. *Phys. Chem. Chem. Phys.* **2001**, *3*, 3955.
(88) Becke, A. D. *J. Chem. Phys.* **1993**, *98*, 1372.
(89) Lee, C. T.; Yang, W. T.; Parr, R. G. *Phys. Rev. B* **1988**, *37*, 785.
(90) Pople, J. A.; Head-Gordon, M.; Raghavachari, K. *J. Chem. Phys.* **1987**, *87*, 5968.
(91) Foresman, J. B.; Frisch, A. E. *Exploring Chemistry with Electronic Structure Methods*, 2nd ed.; Gaussian, Inc.: Pittsburgh, PA, 1996.
(92) *Thermodynamic Properties of Individual Substances*; Gurvich, L. V., Veyts, I. V., Alcock, C. B., Eds.; Hemisphere: New York, 1992; Vol. 2.
(93) Chase, M. W., Jr. *J. Phys. Chem. Ref. Data* **1998**, *monograph 9*, 1.
(94) Hudgens, J. W.; Johnson, R. D. I.; Timonen, R. S.; Seetula, J. A.; Gutman, D. *J. Phys. Chem.* **1991**, *95*, 4400.
(95) Seetula, J. A. *J. Chem. Soc., Faraday Trans.* **1996**, *92*, 3069.
(96) Seetula, J. A.; Russell, J. J.; Gutman, D. *J. Am. Chem. Soc.* **1990**, *112*, 1347.
(97) Kerr, J. A. *CRC Handbook of Chemistry and Physics*, 75th ed.; Lide, D. R., Ed.; CRC Press: Boca Raton, FL, 1995.
(98) Shimanouchi, T. *Tables of Molecular Vibrational Frequencies*; National Bureau of Standards: Gaithersburg, MD, 1972; Consolidated Vol. I.
(99) Andrews, L.; Smith, D. W. *J. Chem. Phys.* **1970**, *53*, 2956.
(100) Carver, T. G.; Andrews, L. *J. Chem. Phys.* **1969**, *50*, 4235.
(101) Jacox, M. E.; Milligan, D. E. *J. Chem. Phys.* **1970**, *53*, 2688.
(102) Russell, J. J.; Seetula, J. A.; Senkan, S. M.; Gutman, D. *Int. J. Chem. Kinet.* **1988**, *20*, 759.